Published in final edited form as:
Nat Genet. 2012 November ; 44(11): 1243–1248. doi:10.1038/ng.2414.

Mutations in *ADAR1* cause Aicardi-Goutières syndrome associated with a type I interferon signature

A full list of authors and affiliations appears at the end of the article.

Abstract

Adenosine deaminases acting on RNA (ADARs) catalyze the hydrolytic deamination of adenosine to inosine in double-stranded RNA (dsRNA) and thereby potentially alter the information content and structure of cellular RNAs. Notably, although the overwhelming majority of such editing events occur in transcripts derived from Alu repeat elements, the biological function of non-coding RNA editing remains uncertain. Here, we show that mutations in *ADAR1* (also known as *ADAR*) cause the autoimmune disorder Aicardi-Goutières syndrome (AGS). As in *Adar1*-null mice, the human disease state is associated with upregulation of interferon-stimulated genes, indicating a possible role for ADAR1 as a suppressor of type I interferon signaling. Considering recent insights derived from the study of other AGS-related proteins, we speculate that ADAR1 may limit the cytoplasmic accumulation of the dsRNA generated from genomic repetitive elements.

Aicardi-Goutières syndrome (MIM 225750) is a genetically determined inflammatory disorder particularly affecting the brain and skin. In its most characteristic form, AGS is a clinical mimic of *in utero*–acquired infection[1] and, like congenital infection, is associated with increased production of the antiviral cytokine interferon α (IFN-α)[2]. AGS can result from mutations in any one of the genes encoding the DNA exonuclease TREX1 (AGS1)[3], the three non-allelic components of the RNase H2 endonuclease complex (RNASEH2B, AGS2; RNASEH2C, AGS3; and RNASEH2A, AGS4)[4] and the deoxynucleoside triphosphate triphosphohydrolase SAMHD1 (AGS5)[5,6]. Although AGS is most typically inherited as an autosomal recessive trait[7], rare examples of disease due to *de novo* dominant mutations in *TREX1* have been reported[8-10].

Correspondence should be addressed to Y.J.C. (yanickcrow@mac.com).

Note: Supplementary information is available in the online version of the paper.

AUTHOR CONTRIBUTIONS

G.I.R. performed quantitative PCR analysis. P.R.K. performed protein blot analysis. G.M.A.F. performed cell culture and interferon stimulation experiments with assistance from G.I.R. and T.A.B. M.S. performed Sanger sequencing with assistance from M.Z., G.M.A.F. and E.M.J. G.I.R. analyzed sequence data. M.S. and G.M.A.F. undertook microsatellite genotyping. J.E.D. and S.S.B. undertook analysis of the exome sequence data. J.H.L. was responsible for neuroradiological phenotyping. P.L. and F.R. measured interferon activity in affected individuals. M.A.O., L.P.K., S.M.G. and N.M.M. carried out ADAR1 editing assays. T.S. and M.K. provided the DSH RNA samples. S.C.L. and P.J.M. carried out ADAR1 structural analysis. Y.J.C. designed and supervised the project and wrote the manuscript with support from G.I.R. C.A.B., R.B., E.B., P.A.B., L.A.B., M.C., C.D.L., P.d.L., M.d.T., I.D., E.F., A.G.-C., A.H., R.K., J.-P.S.-M.L., C.M.L., A.M.M., W.M., C.M., I.O., S.O., P.P., M.R., R.A.R., J.L.S., K.S., T.Y.T., W.G.v.d.M., A.V., G.V., E.L.W., E. Wassmer and E. Whittaker identified subjects with AGS or assisted with related clinical and laboratory studies.

COMPETING FINANCIAL INTERESTS

The authors declare no competing financial interests.

Studies of the function of TREX1 have delineated a cell-intrinsic mechanism for the initiation of an autoimmune response by interferon (IFN)-stimulatory nucleic acid[11,12], begging the question of the source of nucleic acid inducing the type I IFN–mediated immune disturbance in AGS. In this regard, it has been shown that TREX1 can metabolize reverse-transcribed DNA and that single-stranded DNA derived from endogenous retroelements accumulates in TREX1-deficient cells[11]. On a related note, TREX1 (ref. 13), SAMHD1 (refs. 14–16) and RNase H2 (ref. 17) have been implicated in the metabolism of the (exogenous) retrovirus HIV-1. Perhaps most notably, a recent study showed rescue of the lethal inflammatory TREX1-null mouse phenotype by a combination of reverse transcriptase inhibitors (antiretroviral therapy as used to treat HIV-1)[18], suggesting that the accumulation of cytosolic DNA in TREX1-null cells can be ameliorated by inhibiting endogenous retroelement cycling.

To define other genes relevant to the AGS phenotype, we undertook whole-exome sequencing in four individuals with a clinical diagnosis of AGS, all of whom screened negative for mutations in *TREX1*, *RNASEH2A*, *RNASEH2B*, *RNASEH2C* and *SAMHD1*. Using in-solution hybridization followed by massively parallel sequencing, we derived over 2 Gb of mapped sequence for each subject, such that an average of 56-fold coverage was achieved across the exome for all the samples (**Supplementary Table 1**). We performed an analysis of the called nonsynonymous, splice-site, substitution and coding insertion and/or deletion exome variants under a model of a rare autosomal recessive disorder. Visual inspection of the generated data identified two affected individuals, AGS81_P1 and AGS219, who each had two nonsynonymous coding alterations in *ADAR1*, a gene we had already highlighted as a candidate for AGS in view of its known role as a suppressor of type I IFN signaling[19,20]. Sanger sequencing confirmed the variants in these individuals, as well as in two further affected siblings from family AGS81. In light of these data, we proceeded to sequence *ADAR1* in other individuals lacking mutations in *TREX1*, *RNASEH2B*, *RNASEH2C*, *RNASEH2A* and *SAMHD1* (*AGS1–AGS5*, respectively) from our AGS cohort.

In total, 12 affected individuals from 8 families harbored biallelic *ADAR1* variants (**Fig. 1**, **Table 1** and **Supplementary Table 2**), which were considered likely pathogenic on the basis of species conservation (**Supplementary Figs. 1** and **2**) and the output of pathogenicity prediction packages (**Supplementary Table 3**). In these families, all parents tested were heterozygous for one putative mutation. Two further unrelated affected individuals, AGS150 and AGS474, harbored a single mutation encoding p.Gly1007Arg that was not present in either parent. Genotyping of microsatellite markers was consistent with stated paternity, indicating that this variant had arisen *de novo* in both cases (**Supplementary Table 4**). Of the nine distinct *ADAR1* mutations we identified, the c. 577C>G (p.Pro193Ala) transversion was seen in the compound heterozygous state in five families of European ancestry. This same variant was observed in 41 subjects (32 of 4,350 European-Americans and 9 of 2,203 African-Americans) annotated on the Exome Variant Server database, whereas none of the other *ADAR1* variants present in our AGS cohort were found in more than 12,000 control alleles.

ADARs catalyze the hydrolytic deamination of adenosine to inosine in dsRNA[21]. Four ADARs have been described in mammals (ADAR1, ADAR2, ADAR3 and TENR),

although only ADAR1 and ADAR2 are known to have catalytic activity. ADAR1 is encoded by a single-copy gene that maps to human chromosome 1q21. Two main isoforms of ADAR1 are present in mammalian cells: a truncated ADAR1 protein (p110; nucleotide, NM_001025107.2; protein, NP_001020278.1) is constitutively expressed, whereas a full-length form of ADAR1 (p150; nucleotide, NM_001111.4; protein, NP_001102.2) is IFN inducible[22]. Both isoforms have been shown to shuttle between the nucleus and the cytoplasm. ADAR1 is a modular protein with a C-terminal deaminase catalytic domain, three centrally located dsRNA-binding domains (dsRBDs) and one or two N-terminal Z-DNA–binding domains; compared with p110, the p150 isoform of human ADAR1 possesses an additional 295 N-terminal amino acids containing a nuclear export signal and an extra Z-DNA/Z-RNA–binding domain (designated Zα) (**Fig. 1**)[23].

Of the eight amino-acid substitutions identified in our AGS cohort, seven involve residues situated in the catalytic domain of ADAR1 (**Fig. 2**). Five of these seven catalytic domain residues (Arg892, Lys999, Gly1007, Tyr1112 and Asp1113) lie along the surface of the protein that interacts with dsRNA (**Fig. 2a**), and the two others (Ala870 and Ile872) lie internal to the domain structure and are predicted to destabilize the protein (**Fig. 2b,c**). In contrast, Pro193 is positioned within the Z-DNA/Z-RNA–binding domain. In the wild-type protein, Pro193 makes direct contact with the nucleic acid, and substitution of this residue with alanine removes important atomic interactions between the protein and DNA/RNA (**Fig. 2d,e**).

More than 130 different *ADAR1* mutations (**Supplementary Table 5**) have already been documented in individuals with dyschromatosis symmetrica hereditaria 1 (DSH), an autosomal dominant disorder characterized by the childhood onset of hypo- and hyperpigmented macules on the face and dorsal aspects of the extremities[24,25]. The frequent observation of stop and frameshift *ADAR1* variants in individuals with DSH indicates haploinsufficiency as the likely molecular pathology. However, *ADAR1* missense variants, spread throughout the gene, are also commonly seen in association with the DSH phenotype. All except one of the *ADAR1* mutations recorded in our AGS cohort were missense variants, and protein blotting of lymphoblastoid cells from affected individuals showed normal levels of both the constitutive and IFN-inducible isoforms of ADAR1 (**Fig. 3**). We predict that the proteins containing the amino-acid alterations seen in individuals with AGS act as hypomorphs and that, as in the *Adar1*-null mouse, complete loss of ADAR1 protein activity is embryonic lethal[19].

Of the nine discrete *ADAR1* mutations observed in our AGS cases, only the allele encoding p.Gly1007Arg has been reported previously[26,27]. Uniquely, this mutation was described in two individuals with DSH also demonstrating neurodegeneration with dystonia and intracranial calcification (**Supplementary Table 6**). Using a known ADAR1 editing substrate, miR376-a2, we found that, of six ADAR1 p110 mutants (Ala870Thr, Ile872Thr, Arg892His, Lys999Asn, Gly1007Arg and Asp1113His) expressed following transfection of plasmid constructs into HEK293 cells, only the Gly1007Arg variant showed a significant effect on editing, with levels of editing equivalent to those seen with inactive protein (**Fig. 4a**). Modeling to position the deaminase domain active site at the target adenosine along the dsRNA substrate (**Fig. 2f**) predicts that the deaminase domain also contacts dsRBD2 close

to Gly1007. The proximity of Gly1007 to the RNA backbone, and the possibility for an arginine residue to make polyvalent interactions there, suggests a mechanism whereby Arg1007 might confer a dominant-negative effect: by binding more tightly to RNA, the mutant protein could act as a competitive inhibitor of wild-type protein, while being itself catalytically inactive. In keeping with this model, a plasmid expressing Gly1007Arg ADAR1 showed stronger inhibition of wild-type ADAR1 than equivalent amounts of a plasmid expressing catalytically inactive ADAR1 (**Fig. 4b**). Although these observations might explain the seemingly unique nature of the Gly1007Arg variant, how the other mutations that were tested in our system cause an aberrant phenotype remains unclear at this time. Possible explanations might relate, for example, to non-editing functions of ADAR1 (ref. 28) or to editing substrate[29] or cell type specificity[19].

The recurrent p.Pro193Ala alteration lies in the Zα DNA/RNA-binding domain, thus implicating the IFN-inducible p150 isoform of ADAR1 in the AGS phenotype. Mice lacking ADAR1 die by around embryonic day 12.5 owing to defective hematopoiesis and wide-spread apoptosis, which are associated with global upregulation of IFN-stimulated genes (ISGs), indicating that ADAR1 acts as a suppressor of type I IFN signaling[19]. In light of these observations, using whole blood from 8 *ADAR1* mutation–positive individuals, we performed quantitative RT-PCR to analyze the mRNA levels of 15 ISGs. Compared to nine controls, all tested individuals with mutations in *ADAR1*, including AGS150 and AGS474 harboring a *de novo* heterozygous allele encoding p.Gly1007Arg, showed a consistent pattern of ISG upregulation (**Supplementary Fig. 3**). We then undertook an analysis of a subset of the 6 most highly expressed ISGs in 10 *ADAR1* mutation–positive AGS cases, 6 sets of parents with heterozygous mutations in *ADAR1* and 18 *ADAR1* mutation–positive individuals with DSH (**Fig. 5** and **Supplementary Table 7**). For the six ISGs assayed, expression was variably higher in AGS heterozygous parents and DSH cases versus controls, whereas individuals with a clinical diagnosis of AGS (due either to biallelic mutations in *ADAR1* or a heterozygous mutation resulting in a p.Gly1007Arg amino-acid substitution) had even higher levels of expression.

The skin lesions typical of DSH have not been described in AGS (they are distinct from AGS-related chilblains)[30], and none of the *ADAR1* mutation–positive AGS cases included in our study had obvious features of DSH. Of note, DSH has only very rarely been reported outside of Japan and China. Moreover, even within known families segregating the DSH phenotype, a marked variability in expression is well recognized[31]. Although our findings do not necessarily implicate dysregulation of type I IFN in the DSH phenotype, they suggest that missense and null heterozygous mutations in *ADAR1* are consistent with both DSH (depending on, for example, ancestry) and with carrier or, in the case of the p.Gly1007Arg alteration, affected status for AGS. Thus, we believe that the lack of DSH skin features in our AGS cases and their heterozygous parents most likely relates to non-penetrance and/or variable expressivity due to ancestry or other genetic or non-genetic factors, and we predict that two individuals with DSH would have a 1 in 4 risk of having a child with AGS.

Because inosine is recognized as guanosine by the translation and splicing machineries, editing of adenosine to inosine can alter the protein-coding information of messenger RNA and the structural stability of dsRNA. The first identified ADAR-edited substrates were in

codons, and ADARs were presumed to function primarily in proteome diversification. However, although codon editing is clearly important, it represents only a small fraction of editing events in the transcriptome, with editing sites in RNA derived from non-coding regions, most particularly Alu elements, being vastly more prevalent[32-35]. The biological function of such repetitive element editing is uncertain[36]. Recent studies have highlighted an antagonistic interaction between ADARs and the RNA interference machinery, suggesting that a pool of common RNA substrates is capable of engaging both pathways[37] and specifically implicating the binding properties of the p150 isoform of ADAR1, beyond its editing activity[28,38], in this relationship. How, then, does loss of ADAR1 activity lead to upregulation of type I IFN signaling? Theoretically, wild-type ADAR1 might edit specific currently undefined transcripts that are important in IFN regulation. Alternatively, and perhaps more likely, lack of editing in ADAR1-deficient cells may lead to an increase in immunoreactive dsRNA[37] and/or result in failure to generate inosine:uracil (IU)-dsRNA with an intrinsic function in suppressing IFN induction[39]. Considering insights derived from the study of TREX1, SAMHD1 and RNase H2, we speculate that ADAR1 has a role in the metabolism of retroelements and that a major contribution of ADARs to evolutionary fitness may be to regulate the accumulation of dsRNA generated from basally transcribed repetitive sequences within the genome.

URLs. UCSC Human Genome Browser, http://genome.ucsc.edu/; Ensembl, http://www.ensembl.org/; dbSNP, http://www.ncbi.nlm.nih.gov/projects/SNP/; Exome Variant Server, National Heart, Lung, and Blood Institute (NHLBI) Exome Sequencing Project (ESP) (accessed 21 March 2012), http://snp.gs.washington.edu/EVS/; PolyPhen, http://genetics.bwh.harvard.edu/pph/; SIFT, http://sift.jcvi.org/www/SIFT_enst_submit.html; Align GVGD, http://agvgd.iarc.fr/index.php; Clustal Omega, http://www.ebi.ac.uk/Tools/msa/clustalo/; Protein Data Bank (PDB), http://www.pdb.org/; Alamut, http://www.interactive-biosoftware.com/.

ONLINE METHODS

Affected individuals and families

All affected individuals included in this study had a clinical diagnosis of AGS that was based on the presence of early-onset encephalopathy (at <18 months of age), negative investigations for common prenatal infections, intracranial calcification with or without white matter changes in a typical distribution, elevated levels of IFN-α with or without pterins in the cerebrospinal fluid and/or chilblains. Clinical information and samples were obtained with informed consent. The study was approved by the Leeds (East) Research Ethics Committee (reference 10/H1307/132).

Exome sequencing

Genomic DNA was extracted from lymphocytes from affected individuals and parents by standard techniques. For whole-exome analysis, targeted enrichment and sequencing were performed on 3 μg of DNA extracted from the peripheral blood of four individuals (AGS81_P1, AGS125, AGS163 and AGS219). Enrichment was undertaken using the 38 Mb SureSelect Human All Exon kit (Agilent) following the manufacturer's protocol, and

samples were paired-end sequenced on an Illumina HiSeq 2000. Sequence data were mapped using BWA (Burrows-Wheeler Aligner) against the hg18 (NCBI Build 36) human genome as a reference. Variants were called using SOAPsnp and SOAPindel (from the Short Oligonucleotide Analysis Package) with medium stringency and were then filtered for those with greater than 5× coverage.

Sanger sequencing

Primers were designed to amplify the coding exons of *ADAR1* (**Supplementary Table 8**). Purified PCR amplification products were sequenced using BigDye terminator chemistry and an ABI 3130 DNA sequencer. Mutations were annotated on the basis of the reference cDNA sequence NM_001111.4, with nucleotide numbering beginning from the first A in the initiating ATG codon.

Gene expression analysis

The expression of 15 genes known to be interferon stimulated was assessed in whole blood. Total RNA was extracted from whole blood using the PAXgene RNA isolation kit (PreAnalytix). RNA concentration was assessed using a spectrophotometer (FLUOstar Omega, Labtech). Quantitative RT-PCR analysis was performed using TaqMan Universal PCR Master Mix (Applied Biosystems) and cDNA derived from 40 ng of total RNA. The relative abundance of target transcripts, measured using TaqMan probes for *Ly6E* (Hs00158942_m1), *MX1* (Hs00895598_m1), *USP18* (Hs00276441_m1), *RSAD2* (Hs01057264_m1), *OAS1* (Hs00973637_m1), *IFI44L* (Hs00199115_m1), *IFI27* (Hs01086370_m1), *ISG15* (Hs00192713_m1), *IFIT1* (Hs00356631_g1), *IFI44* (Hs00197427_m1), *IFI6* (Hs00242571_m1), *SIGLEC1* (Hs00988063_m1), *IFIT3* (Hs00155468_m1), *IRF7* (Hs00185375_m1) and *STAT1* (Hs01013989_m1), was normalized to the expression level of *HPRT1* (Hs03929096_g1) and *18s* (Hs999999001_s1) and assessed with Applied Biosystems StepOne Software v2.1. Statistical significance between groups was determined by *t* tests using DataAssist v2.0 (Applied Biosystems). Data from affected individuals are expressed relative to the average of nine normal controls. A subset of the six most highly expressed ISGs (*RSAD2*, *IFI44L*, *IFI27*, *ISG15*, *IFIT1* and *SIGLEC1*) were measured in 20 controls, 10 *ADAR1* mutation–positive cases, 6 sets of *ADAR1* heterozygous parents and 18 individuals with *ADAR1* mutation–positive DSH. RNA from individuals with DSH was extracted using the QIAamp RNA Blood Mini kit (Qiagen), and cDNA was derived as above. Statistical significance between groups was determined by Kruskall Wallis tests using GraphPad Prism 5. The median fold change of the 6 ISGs compared to the median of the 20 healthy controls was used to create a score for each affected individual, similarly to previously described methods[41,42].

Interferon stimulation

EBV-transformed lymphoblastoid cells from affected individuals and controls were counted using a Bright-Line Hemacytometer (Sigma). We then transferred 10 ml of cells at a concentration of 1×10^6 cells/ml to each of two T25 flasks per cell line. One flask for each cell line was stimulated with 1,000 international units (IU)/ml of human IFN-α (human Intron A, Shering-Plough) for 24 h.

Protein analysis

Whole-cell lysates were prepared from lymphoblastoid cells (1×10^7 cells per sample) using 10 mM EDTA–RIPA buffer containing protease inhibitors (Roche). For protein blot analysis, 10 μg of total protein was loaded onto 8% SDS-PAGE gels, and electrophoresis was performed using the Mini-PROTEAN system (Bio-Rad Laboratories). Following wet-blotting transfer of the proteins onto PVDF membrane (Amersham), non-specific antibody binding was blocked using 5% normal goat serum (Vector Laboratories) and 2% BSA (Sigma) in 0.1% TBS-Tween (Sigma) overnight at 4 °C with gentle agitation. Rabbit primary antibody to ADAR (Sigma, Prestige Antibodies, HPA003890) was incubated with the membranes for 2 h at room temperature using a dilution of 1:800. As a loading control, membranes were incubated with a 1:4,000 dilution of rabbit primary antibody to α/β-tubulin (Cell Signaling Technology, 2148). Horseradish peroxidase (HRP)-labeled goat secondary antibody to rabbit (1:10,000; Cell Signaling Technology, 7074) was incubated with the membranes for 1 h at room temperature to detect both ADAR1 and tubulin antibodies. Signal was detected using a 1:10 dilution of Enhanced Chemiluminescence reagents (Lumigen).

Microsatellite genotyping

To exclude non-paternity, informative polymorphic microsatellite markers on chromosomes 3 (D3S3640 and D3S3560), 11 (D11S913 and D11S1889) and 20 (D20S847, D20S896 and D20S843) were genotyped using DNA from AGS150, AGS475, their parents and an unrelated control sample. DNA samples were amplified by standard PCR (primer sequences available upon request). Each amplicon was mixed with Hi-Di Formamide (Applied Biosystems) and 500 ROX Size Standard (Applied Biosystems) and run on the Genetic Analyzer 3010 capillary electrophoresis system. Results were analyzed with GeneMapper v4.1 software (Applied Biosystems).

Editing assays

Transient transfections were performed with slight adaptations to a previously described protocol[28] in 24-well plates seeded the day before transfection with 0.14×10^6 cells using Lipofectamine 2000 and OptiMEM I reduced serum medium. Cells were transfected with 500 ng of plasmid expressing a known ADAR1 editing substrate, miR376-a2, together with 500 ng of plasmid expressing wild-type ADAR1 p110 protein or the mutants Ala870Thr, Ile872Thr, Arg892His, Lys999Asn, Gly1007Arg and Asp1113His, for which coding sequences had been subcloned into the pcDNA3.1 expression vector. Reduced serum medium was replaced after 6 h with DMEM, and cells were harvested after 48 h. Total RNA was extracted with TRIzol reagent (Invitrogen), purified and treated with TURBO DNase (Ambion) and RNasin Plus RNase Inhibitor (Promega). Reverse transcription was carried out using SuperScript II and random hexamers, and cDNA was amplified by PCR with Platinum Taq DNA polymerase and specific primers for pri-miR376-a2 (**Supplementary Table 8**). The 300-bp PCR product was purified with exonuclease in combination with shrimp alkaline phosphatase (SAP) before sequencing. RNA editing of the pri-miR376-a2 transcript was identified as an adenosine-to-guanine change within the cDNA sequence, and the editing level was expressed as a percentage. Peak heights were measures for edited (G)

and unedited (A), the editing ratio percentage was calculated by (G / (A + G)) × 100. Results are the average of two separate experiments. Statistical significance between groups was determined by two-tailed *t* tests using Excel.

Protein modeling

The ADAR1 substitutions p.Ala870Thr, p.Ile872Thr, p.Arg892His, p.Lys999Asn, p.Gly1007Arg, p.Tyr1112Phe and p.Asp1113His all fall within the adenosine deaminase domain. No crystal structure is available for this domain in human ADAR1; thus, a comparative model was constructed using the deaminase domain of human ADAR2 (Protein Data Bank (PDB) 1zy7)[43]. The sequences of ADAR1 and ADAR2 were aligned using ClustalW[44], and 25 models were built using Modeller[45]. The model with the lowest discrete optimized protein energy (DOPE) score was selected (representing the most probable model judged by the fit to the Modeller statistical potential). Residues 975–996 could not be modeled accurately, as they have no equivalent in ADAR2; for this reason, these residues were not analyzed further. Models of mutations were built using KiNG[46], hydrogen atoms were added with Reduce[47], and all-atom contacts were calculated with Probe[48]. In each case, all low-energy rotamers[49] were considered, and the rotamer with the best Probe score was used. We assumed a similar binding mode for ADAR2 to that described for the tRNA deaminase–tRNA anticodon complex[50], allowing us to orientate the deaminase domain of ADAR2 on dsRNA and position it relative to the ADAR2-dsRBD2 complex[51]. The crystal structure of the ADAR1 Z-DNA–binding domain[52] (PDB 1qbj) was used to analyze the likely structural effect of the p.Pro193Ala substitution. As the side chain of alanine has no degrees of freedom from rotatable dihedral angles, the position of the side chain is determined by the conformation of the protein backbone.

Supplementary Material

Refer to Web version on PubMed Central for supplementary material.

Authors

Gillian I Rice[1], Paul R Kasher[1], Gabriella M A Forte[1], Niamh M Mannion[2], Sam M Greenwood[2], Marcin Szynkiewicz[1], Jonathan E Dickerson[1], Sanjeev S Bhaskar[1], Massimiliano Zampini[1], Tracy A Briggs[1], Emma M Jenkinson[1], Carlos A Bacino[3], Roberta Battini[4], Enrico Bertini[5], Paul A Brogan[6], Louise A Brueton[7], Marialuisa Carpanelli[8], Corinne De Laet[9], Pascale de Lonlay[10], Mireia del Toro[11], Isabelle Desguerre[12], Elisa Fazzi[13], Àngels Garcia-Cazorla[14,15], Arvid Heiberg[16], Masakazu Kawaguchi[17], Ram Kumar[18], Jean-Pierre S-M Lin[19], Charles M Lourenco[20], Alison M Male[21], Wilson Marques Jr[20], Cyril Mignot[22,24], Ivana Olivieri[25], Simona Orcesi[25], Prab Prabhakar[26], Magnhild Rasmussen[27], Robert A Robinson[26], Flore Rozenberg[28], Johanna L Schmidt[29], Katharina Steindl[30], Tiong Y Tan[31], William G van der Merwe[32], Adeline Vanderver[29], Grace Vassallo[33], Emma L Wakeling[34], Evangeline Wassmer[35], Elizabeth Whittaker[36], John H Livingston[37], Pierre Lebon[28], Tamio Suzuki[17], Paul J McLaughlin[38], Liam P Keegan[2], Mary A O'Connell[2], Simon C Lovell[39], and Yanick J Crow[1]

Affiliations

[1]Manchester Academic Health Science Centre, University of Manchester, Genetic Medicine, Manchester, UK [2]Medical Research Council (MRC) Human Genetics Unit, Institute of Genetics and Molecular Medicine (IGMM), University of Edinburgh, Edinburgh, UK [3]Department of Molecular and Human Genetics, Baylor College of Medicine, Houston, Texas, USA [4]Department of Developmental Neuroscience, Istituto di Ricovero e Cura a Carattere Scientifico (IRCCS) Stella Maris, Pisa, Italy [5]Laboratory of Molecular Medicine, Department of Neuroscience, Bambino Gesù Children's Research Hospital, Rome, Italy [6]University College London (UCL) Institute of Child Health, London, UK [7]Birmingham Women's National Health Service (NHS) Foundation Trust, Birmingham, UK [8]Department of Child Neurology and Psychiatry, A Manzoni Hospital, Lecco, Italy [9]Nutrition and Metabolism Unit, Hôpital Universitaire des Enfants Reine Fabiola (ULB), Brussels, Belgium [10]Reference Center of Metabolic Diseases, Hôpital Necker–Enfants Malades, Paris Descartes University, Paris, France [11]Pediatric Neurology Unit, Hospital Vall d'Hebron, Barcelona, Spain [12]Neuropediatric Unit, Assistance Publique–Hôpitaux de Paris (AP-HP), Paris V Descartes University, Necker Hospital, Paris, France [13]Mother and Child Department, Unit of Child Neurology and Psychiatry, Civil Hospital, University of Brescia, Brescia, Italy [14]Department of Neurology, Hospital Sant Joan de Déu (HSJD), Barcelona, Spain [15]El Centro de Investigación Biomédica en Red de Enfermedades Raras (CIBER-ER), Instituto de Salud Carlos III, Madrid, Spain [16]Department of Medical Genetics, Oslo University Hospital, National Hospital, Oslo, Norway [17]Department of Dermatology, Yamagata University Faculty of Medicine, Yamagata, Japan [18]Department of Neurology, Alder Hey Children's NHS Foundation Trust, Liverpool, UK [19]General Neurology & Complex Motor Disorders Service, Evelina Children's Hospital, Guy's & St. Thomas' NHS Foundation Trust, London, UK [20]Department of Neurosciences and Behavior Sciences, School of Medicine of Ribeirão Preto, University of São Paulo, São Paulo, Brazil [21]North East Thames Regional Genetics Service, Great Ormond Street Hospital for Children, London, UK [22]Département de Génétique et Cytogénétique, AP-HP, Groupe Hospitalier Pitié–Salpêtrière, Paris, France [23]Service de Neuropédiatrie, AP-HP, Hopital Armand Trousseau, Paris, France [24]Centre de Déficience des Déficiences Intellectuelles de Causes Rares, Paris, France [25]Child Neurology and Psychiatry Unit, IRCCS C Mondino National Institute of Neurology Foundation, Pavia, Italy [26]Department of Neurology, Great Ormond Street Hospital, London, UK [27]Section of Child Neurology, Women and Children's Division, Oslo University Hospital, Oslo, Norway [28]Service de Virologie, Paris Descartes University, AP-HP, Hopital Cochin St. Vincent de Paul, Paris, France [29]Department of Neurology, Children's National Medical Center, Washington, DC, USA [30]Institute of Medical Genetics, University of Zurich, Schwerzenbach, Switzerland [31]Victorian Clinical Genetics Services, Murdoch Children's Research Institute, Royal Children's Hospital, Melbourne, Victoria, Australia [32]Paediatric Department, Nobles Hospital, Strang, UK [33]Neurology Department, Royal Manchester Children's Hospital, Manchester, UK [34]North West Thames Regional

Genetics Service, North West London Hospitals NHS Trust, Harrow, UK
[35]Neurology Department, Birmingham Children's Hospital, Birmingham, UK
[36]Academic Department of Paediatrics, Imperial College London, London, UK
[37]Department of Paediatric Neurology, Leeds General Infirmary, Leeds, UK
[38]Institute of Structural and Molecular Biology, School of Biological Sciences, The University of Edinburgh, Edinburgh, UK [39]Faculty of Life Sciences, University of Manchester, Manchester, UK

Acknowledgments

We sincerely thank the participating families for the use of genetic samples and clinical information. We thank B. Hamel, H. Brunner and other clinical collaborators for contributing samples not included in the current manuscript, A.P. Jackson for highlighting the presence of intracranial calcification in individuals with DSH with a p.Gly1007Arg alteration in ADAR1 and D.B. Stetson and D.T. Bonthron for critical reading of the manuscript. D.B. Stetson (University of Washington) provided the *ADAR1* constructs used in the editing assays. We thank the NHLBI GO Exome Sequencing Project and its ongoing studies that produced and provided exome variant calls for comparison: the Lung GO Sequencing Project (HL-102923), the Women's Health Initiative (WHI) Sequencing Project (HL-102924), the Broad GO Sequencing Project (HL-102925), the Seattle GO Sequencing Project (HL-102926) and the Heart GO Sequencing Project (HL-103010). Y.J.C. acknowledges the Manchester National Institute for Health Research (NIHR) Biomedical Research Centre. The research leading to these results has received funding from the European Union's Seventh Framework Programme (FP7/2007-2013) under grant agreement 241779 and from the Great Ormond Street Hospital Children's Charity.

References

1. Crow YJ, Livingston JH. Aicardi-Goutières syndrome: an important Mendelian mimic of congenital infection. Dev. Med. Child Neurol. 2008; 50:410–416. [PubMed: 18422679]
2. Lebon P, et al. Intrathecal synthesis of interferon-α in infants with progressive familial encephalopathy. J. Neurol. Sci. 1988; 84:201–208. [PubMed: 2837539]
3. Crow YJ, et al. Mutations in the gene encoding the 3′-5′ DNA exonuclease TREX1 cause Aicardi-Goutières syndrome at the *AGS1* locus. Nat. Genet. 2006; 38:917–920. [PubMed: 16845398]
4. Crow YJ, et al. Mutations in genes encoding ribonuclease H2 subunits cause Aicardi-Goutières syndrome and mimic congenital viral brain infection. Nat. Genet. 2006; 38:910–916. [PubMed: 16845400]
5. Rice GI, et al. Mutations involved in Aicardi-Goutières syndrome implicate SAMHD1 as regulator of the innate immune response. Nat. Genet. 2009; 41:829–832. [PubMed: 19525956]
6. Goldstone DC, et al. HIV-1 restriction factor SAMHD1 is a deoxynucleoside triphosphate triphosphohydrolase. Nature. 2011; 480:379–382. [PubMed: 22056990]
7. Rice G, et al. Clinical and molecular phenotype of Aicardi-Goutières syndrome. Am. J. Hum. Genet. 2007; 81:713–725. [PubMed: 17846997]
8. Rice G, et al. Heterozygous mutations in *TREX1* cause familial chilblain lupus and dominant Aicardi-Goutières syndrome. Am. J. Hum. Genet. 2007; 80:811–815. [PubMed: 17357087]
9. Ramantani G, et al. Expanding the phenotypic spectrum of lupus erythematosus in Aicardi-Goutières syndrome. Arthritis Rheum. 2010; 62:1469–1477. [PubMed: 20131292]
10. Haaxma CA, et al. A *de novo* p.Asp18Asn mutation in *TREX1* in a patient with Aicardi-Goutières syndrome. Am. J. Med. Genet. A. 2010; 152A:2612–2617. [PubMed: 20799324]
11. Stetson DB, Ko JS, Heidmann T, Medzhitov R. Trex1 prevents cell-intrinsic initiation of autoimmunity. Cell. 2008; 134:587–598. [PubMed: 18724932]
12. Gall A, et al. Autoimmunity initiates in nonhematopoietic cells and progresses via lymphocytes in an interferon-dependent autoimmune disease. Immunity. 2012; 36:120–131. [PubMed: 22284419]
13. Yan N, et al. The cytosolic exonuclease TREX1 inhibits the innate immune response to human immunodeficiency virus type 1. Nat. Immunol. 2010; 11:1005–1013. [PubMed: 20871604]

14. Laguette N, et al. SAMHD1 is the dendritic- and myeloid-cell-specific HIV-1 restriction factor counteracted by Vpx. Nature. 2011; 474:654–657. [PubMed: 21613998]
15. Hrecka K, et al. Vpx relieves inhibition of HIV-1 infection of macrophages mediated by the SAMHD1 protein. Nature. 2011; 474:658–661. [PubMed: 21720370]
16. Lahouassa H, et al. SAMHD1 restricts the replication of human immunodeficiency virus type 1 by depleting the intracellular pool of deoxynucleoside triphosphates. Nat. Immunol. 2012; 13:223–228. [PubMed: 22327569]
17. Genovesio A, et al. Automated genome-wide visual profiling of cellular proteins involved in HIV infection. J. Biomol. Screen. 2011; 16:945–958. [PubMed: 21841144]
18. Beck-Engeser GB, Eilat D, Wabl M. An autoimmune disease prevented by anti-retroviral drugs. Retrovirology. 2011; 8:91. [PubMed: 22067273]
19. Hartner JC, Walkley CR, Lu J, Orkin SH. ADAR1 is essential for the maintenance of hematopoiesis and suppression of interferon signaling. Nat. Immunol. 2009; 10:109–115. [PubMed: 19060901]
20. Crow YJ. Type I interferonopathies: a novel set of inborn errors of immunity. Ann. NY Acad. Sci. 2011; 1238:91–98. [PubMed: 22129056]
21. Hogg M, Paro S, Keegan LP, O'Connell MA. RNA editing by mammalian ADARs. Adv. Genet. 2011; 73:87–120. [PubMed: 21310295]
22. George CX, Samuel CE. Human RNA-specific adenosine deaminase *ADAR1* transcripts possess alternative exon 1 structures that initiate from different promoters, one constitutively active and the other interferon inducible. Proc. Natl. Acad. Sci. USA. 1999; 96:4621–4626. [PubMed: 10200312]
23. Herbert A, et al. A Z-DNA binding domain present in the human editing enzyme, double-stranded RNA adenosine deaminase. Proc. Natl. Acad. Sci. USA. 1997; 94:8421–8426. [PubMed: 9237992]
24. Miyamura Y, et al. Mutations of the RNA-specific adenosine deaminase gene (*DSRAD*) are involved in dyschromatosis symmetrica hereditaria. Am. J. Hum. Genet. 2003; 73:693–699. [PubMed: 12916015]
25. Li M, et al. Mutational spectrum of the *ADAR1* gene in dyschromatosis symmetrica hereditaria. Arch. Dermatol. Res. 2010; 302:469–476. [PubMed: 20186421]
26. Tojo K, et al. Dystonia, mental deterioration, and dyschromatosis symmetrica hereditaria in a family with *ADAR1* mutation. Mov. Disord. 2006; 21:1510–1513. [PubMed: 16817193]
27. Kondo T, et al. Dyschromatosis symmetrica hereditaria associated with neurological disorders. J. Dermatol. 2008; 35:662–666. [PubMed: 19017046]
28. Heale BS, et al. Editing independent effects of ADARs on the miRNA/siRNA pathways. EMBO J. 2009; 28:3145–3156. [PubMed: 19713932]
29. Cho DS, et al. Requirement of dimerization for RNA editing activity of adenosine deaminases acting on RNA. J. Biol. Chem. 2003; 278:17093–17102. [PubMed: 12618436]
30. Abdel-Salam GM, et al. Chilblains as a diagnostic sign of Aicardi-Goutières syndrome. Neuropediatrics. 2010; 41:18–23. [PubMed: 20571986]
31. Kondo T, et al. Six novel mutations of the *ADAR1* gene in patients with dyschromatosis symmetrica hereditaria: histological observation and comparison of genotypes and clinical phenotypes. J. Dermatol. 2008; 35:395–406. [PubMed: 18705826]
32. Levanon EY, et al. Systematic identification of abundant A-to-I editing sites in the human transcriptome. Nat. Biotechnol. 2004; 22:1001–1005. [PubMed: 15258596]
33. Athanasiadis A, Rich A, Maas S. Widespread A-to-I RNA editing of Alu-containing mRNAs in the human transcriptome. PLoS Biol. 2004; 2:e391. [PubMed: 15534692]
34. Blow M, Futreal PA, Wooster R, Stratton MR. A survey of RNA editing in human brain. Genome Res. 2004; 14:2379–2387. [PubMed: 15545495]
35. Kim DD, et al. Widespread RNA editing of embedded Alu elements in the human transcriptome. Genome Res. 2004; 14:1719–1725. [PubMed: 15342557]
36. Hundley HA, Bass BL. ADAR editing in double-stranded UTRs and other noncoding RNA sequences. Trends Biochem. Sci. 2010; 35:377–383. [PubMed: 20382028]

37. Wu D, Lamm AT, Fire AZ. Competition between ADAR and RNAi pathways for an extensive class of RNA targets. Nat. Struct. Mol. Biol. 2011; 18:1094–1101. [PubMed: 21909095]
38. Yang W, et al. ADAR1 RNA deaminase limits short interfering RNA efficacy in mammalian cells. J. Biol. Chem. 2005; 280:3946–3953. [PubMed: 15556947]
39. Vitali P, Scadden AD. Double-stranded RNAs containing multiple IU pairs are sufficient to suppress interferon induction and apoptosis. Nat. Struct. Mol. Biol. 2010; 17:1043–1050. [PubMed: 20694008]
40. Gallo A, Keegan LP, Ring GM, O'Connell MA. An ADAR that edits transcripts encoding ion channel subunits functions as a dimer. EMBO J. 2003; 22:3421–3430. [PubMed: 12840004]
41. Yao Y, et al. Development of potential pharmacodynamic and diagnostic markers for anti–IFN-α monoclonal antibody trials in systemic lupus erythematosus. Hum. Genomics Proteomics. 2009; 2009:374312. [PubMed: 20948567]
42. Higgs BW, et al. Patients with systemic lupus erythematosus, myositis, rheumatoid arthritis and scleroderma share activation of a common type I interferon pathway. Ann. Rheum. Dis. 2011; 70:2029–2036. [PubMed: 21803750]
43. Macbeth MR, et al. Inositol hexakisphosphate is bound in the ADAR2 core and required for RNA editing. Science. 2005; 309:1534–1539. [PubMed: 16141067]
44. Larkin MA, et al. Clustal W and Clustal X version 2.0. Bioinformatics. 2007; 23:2947–2948. [PubMed: 17846036]
45. Sali A, Blundell TL. Comparative protein modelling by satisfaction of spatial restraints. J. Mol. Biol. 1993; 234:779–815. [PubMed: 8254673]
46. Chen VB, Davis IW, Richardson DC. KING (Kinemage, Next Generation): a versatile interactive molecular and scientific visualization program. Protein Sci. 2009; 18:2403–2409. [PubMed: 19768809]
47. Word JM, Lovell SC, Richardson JS, Richardson DC. Asparagine and glutamine: using hydrogen atom contacts in the choice of side-chain amide orientation. J. Mol. Biol. 1999; 285:1735–1747. [PubMed: 9917408]
48. Word JM, et al. Visualizing and quantifying molecular goodness-of-fit: small-probe contact dots with explicit hydrogen atoms. J. Mol. Biol. 1999; 285:1711–1733. [PubMed: 9917407]
49. Lovell SC, Word JM, Richardson JS, Richardson DC. The penultimate rotamer library. Proteins. 2000; 40:389–408. [PubMed: 10861930]
50. Losey HC, Ruthenburg AJ, Verdine GL. Crystal structure of *Staphylococcus aureus* tRNA adenosine deaminase TadA in complex with RNA. Nat. Struct. Mol. Biol. 2006; 13:153–159. [PubMed: 16415880]
51. Stefl R, et al. The solution structure of the ADAR2 dsRBM-RNA complex reveals a sequence-specific readout of the minor groove. Cell. 2010; 143:225–237. [PubMed: 20946981]
52. Schwartz T, et al. Crystal structure of the Zα domain of the human editing enzyme ADAR1 bound to left-handed Z-DNA. Science. 1999; 284:1841–1845. [PubMed: 10364558]

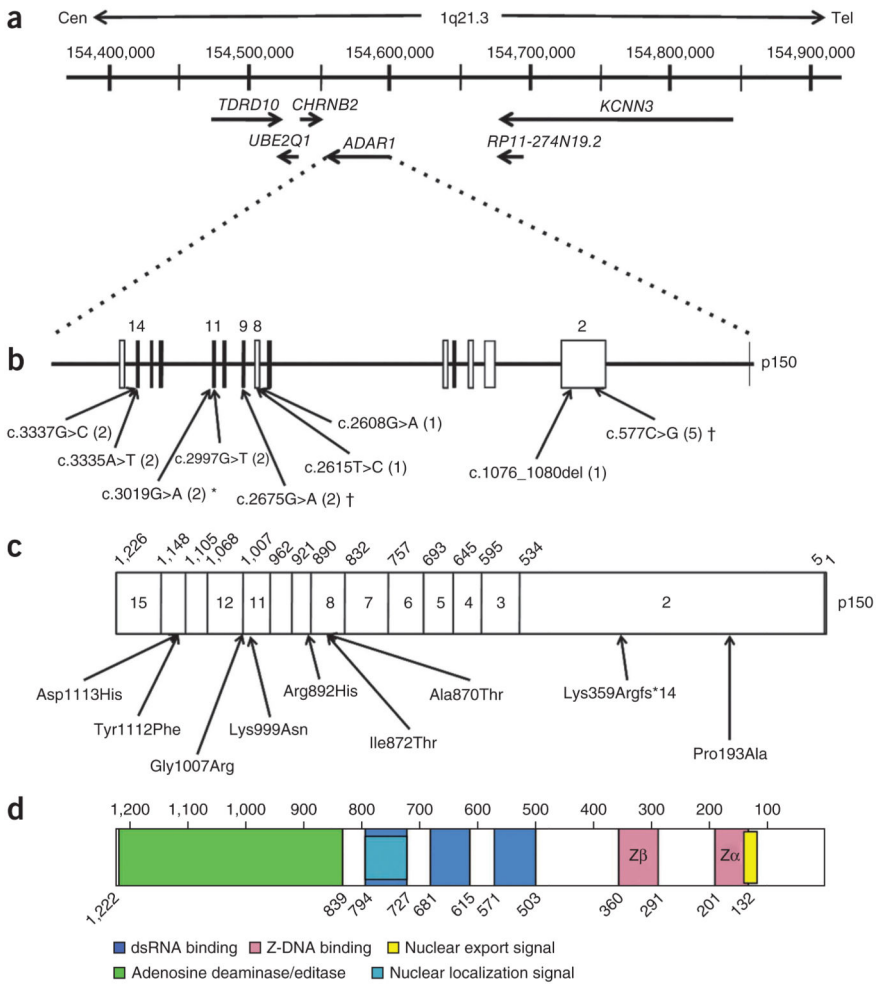

Figure 1.

Schematic of the human *ADAR1* gene. (**a**) *ADAR1* spans 26,191 bp of genomic sequence on chromosome 1q21.3 (154,554,533–154,580,724). Neighboring genes are also shown. Cen, centromeric; tel, telomeric. (**b**) Position of identified mutations within the genomic sequence of the *ADAR1* long isoform (p150). The number of alleles with each mutation is shown in parentheses. *, the mutation encoding p.Gly1007Arg identified as a single heterozygous *de novo* change in two families; †, the same mutation identified in identical twins (therefore counted once). Numbers given above the gene indicate the relevant exons (only exons with mutations are numbered). The shorter isoform (p110) of *ADAR1* starts at c.886 of the p150 isoform. (**c**) Position of identified variants within the ADAR1 p150 1,226-amino-acid protein. Numbers above the protein are the amino-acid count at the exon boundaries. The shorter isoform starts at amino acid 296 of p150, giving rise to a 931-amino-acid protein. (**d**) Schematic of the position of protein domains and their amino-acid boundaries in the p150 isoform of ADAR1. Note that the p110 isoform does not include the Zα DNA/RNA-binding domain and nuclear export signal.

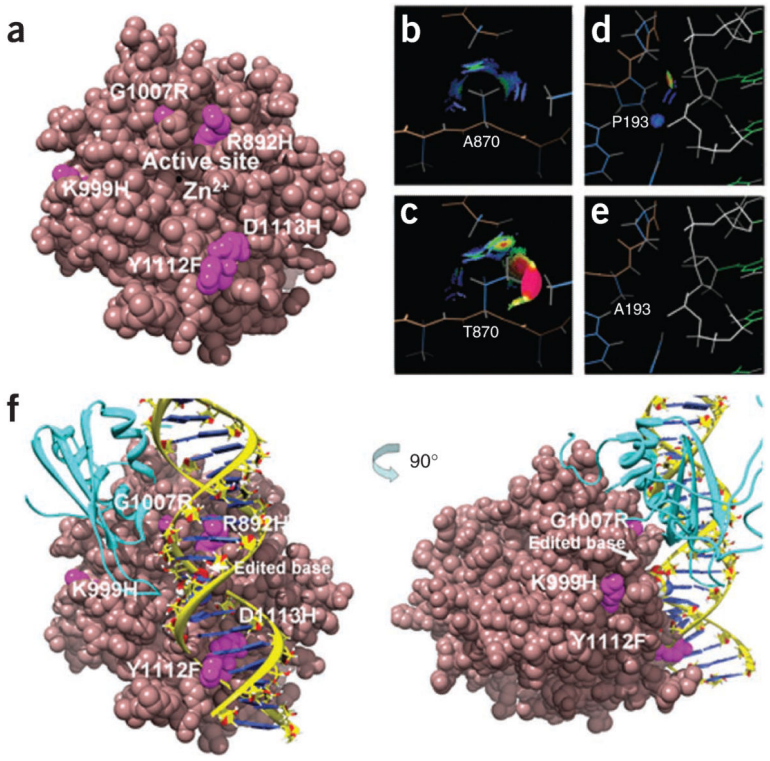

Figure 2.

Structural context of ADAR1 protein substitutions. (**a**) The surface of the ADAR domain (dark pink) with surface substitutions highlighted in bright pink. The active site contains a zinc ion (black) in the center. Arg892His, Lys999Asn, Gly1007Arg, Tyr1112Phe and Asp1113His are all on the same side of the domain as the active site, and all have the potential to alter charge and/or hydrogen bonding characteristics of the surface in the region that is likely to be responsible for RNA binding. (**b**,**c**) Models of wild-type (**b**) and mutant (**c**) residues at position 870 in the ADAR domain. Interactions between the residue and the surrounding protein structure are indicated by all-atom contact dots (blue). Green dots represent energetically favorable van der Waals interactions, whereas red and pink spikes indicate unfavorable van der Waals overlaps. The Ile872Thr substitution introduces an unsatisfied hydrogen bond donor/acceptor group, which is destabilizing but not easily depicted. (**d**,**e**) Interactions of the proline residue at position 193 (Pro193) in the Z-DNA–binding domain (**d**). Contact dots (blue, green, yellow) indicate favorable interactions between Pro193 and the DNA backbone (white). These interactions are absent in the mutant form (**e**). (**f**) Modeling of the deaminase domain of ADAR2 suggests contact with dsRBD2 close to Gly1007, highlighting the possibility for an arginine residue to make functionally important polyvalent interactions.

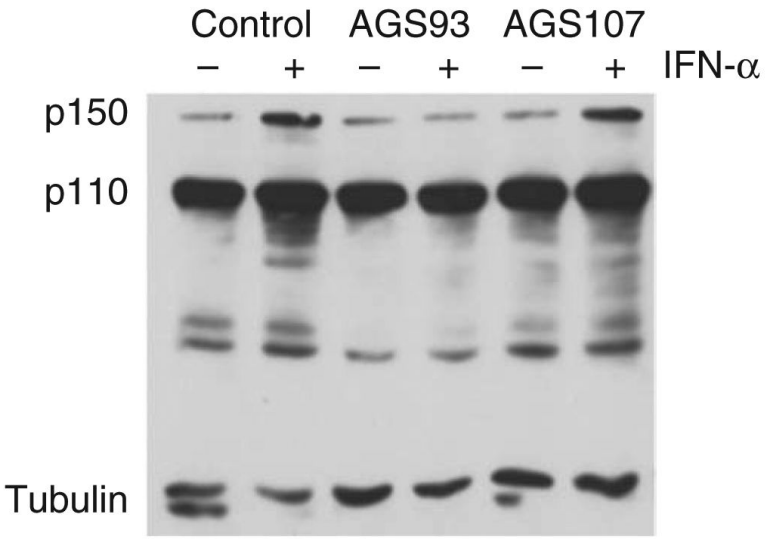

Figure 3.

Protein blot of lymphoblastoid cell lines (LCLs). Protein blot analysis of ADAR1 expression in Epstein-Barr virus (EBV)-transformed LCLs from one unrelated control and two affected individuals (AGS93, AGS107). Whole-cell lysates were derived from 1×10^7 cells per sample, and 10 μg of total protein was loaded per lane. To test antibody specificity and confirm IFN induction of the p150 isoform of ADAR1, unstimulated cells were compared to IFN-stimulated cells. The antibody to ADAR1 recognizes both the p110 and p150 isoforms. Immunoblotting of tubulin (50–55 kDa) was used as a loading control.

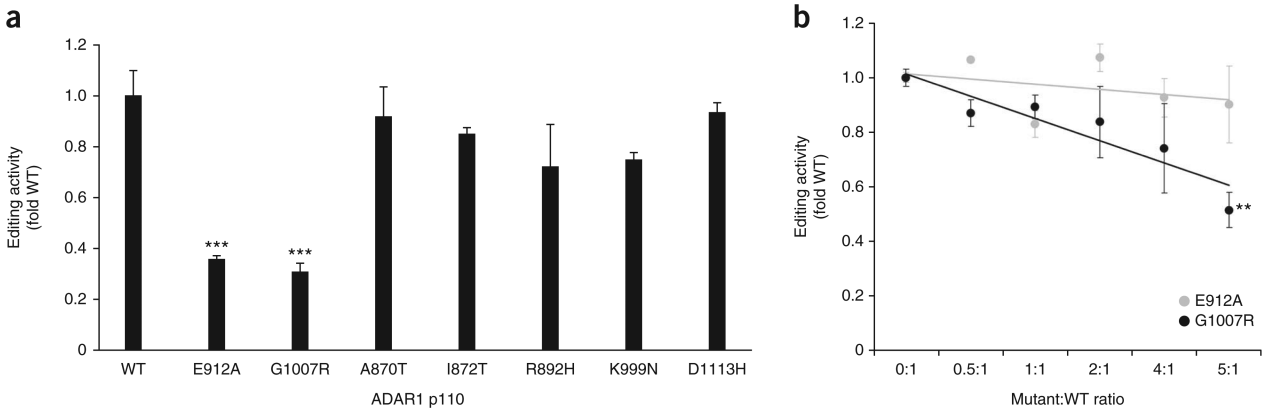

Figure 4.

Site-specific and competition editing assays. (**a**) HEK293 cells were co-transfected with 500 ng of a plasmid expressing miR376-a2 and 500 ng of a plasmid expressing wild-type (WT) ADAR1 or ADAR1 mutants. Background editing in HEK293 cells with 500 ng of substrate plasmid is approximately 20%. As previously observed, only one monomer in an ADAR1 dimer is required to be enzymatically active, such that addition of inactive protein initially increases editing[40]. Editing activity is expressed as a proportion of WT ADAR1 editing activity, which is 1 (*y* axis). Error bars, s.e.m. ****P* = 0.0005. (**b**) Competition between ADAR1 and inactive ADAR1 mutants. HEK293 cells were co-transfected with 200 ng of a plasmid expressing miR376-a2 and 200 ng of a plasmid expressing ADAR1 p110 in the presence of increasing amounts of a plasmid expressing a catalytically inactive form of ADAR1 (Glu912Ala)[28] or Gly1007Arg. Error bars, s.e.m. ***P* = 0.0026.

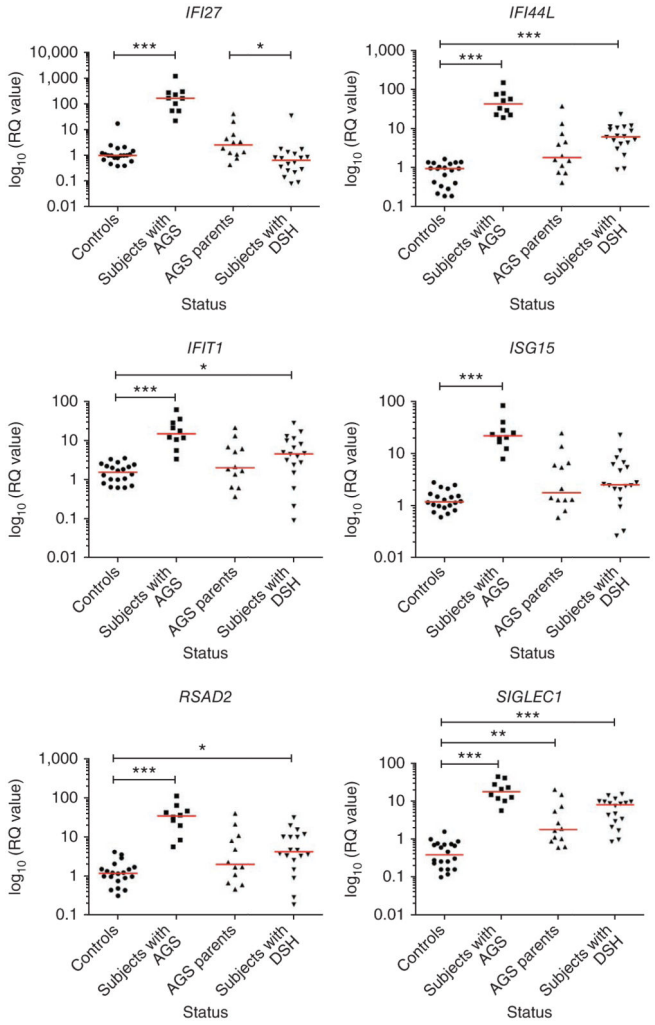

Figure 5.

Quantitative RT-PCR of a panel of six ISGs in whole blood measured in individuals with AGS, their parents and individuals with DSH. Scatter plots showing $\log_{10}$-transformed RQ values for a panel of 6 ISGs measured in whole blood from 10 AGS cases with mutations in *ADAR1*, 6 sets of parents heterozygous for mutations in *ADAR1*, 18 individuals with *ADAR1* mutation–positive DSH and 20 healthy controls. All genes were significantly upregulated in AGS cases ($P < 0.001$) compared to controls. RQ is equal to $2^{-\Delta\Delta C_T}$, with $-\Delta\Delta C_T \pm$ s.d., that is the normalized fold change relative to a calibrator. ***$P \leq 0.001$; **$P \leq 0.01$; *$P < 0.05$.

Table 1

Ancestry, pedigree structure, consanguinity status and sequence alterations in *ADAR1* mutation–positive families in an AGS cohort

Family	Ancestry	Individuals tested	Consanguinity	Nucleotide alteration	Exon	Amino-acid alteration
AGS81	Norwegian	3A, M, F	−	c.[577C>G]+[2675G>A]	2, 9	p.[Pro193Ala]+[Arg892His]
AGS93	Italian	1A, M, F	−	c.[577C>G]+[2608G>A]	2, 8	p.[Pro193Ala]+[Ala870Thr]
AGS107	Pakistani	2A, M, F	+	c.3337G>C (hom)	14	p.Asp1113His
AGS150	Brazilian	1A, M, F	−	c.3019G>A (het, *de novo*)	11	p.Gly1007Arg
AGS219	Pakistani	1A	+	c.3335A>T (hom)	14	p.Tyr1112Phe
AGS228	Indian	1A, M, F	−	c.2997G>T (hom)	11	p.Lys999Asn
AGS251	White British	1A, M	−	c.[577C>G]+[2615T>C]	2, 8	p.[Pro193Ala]+[Ile872Thr]
AGS327	Italian	1A	−	c.[577C>G]+[1076_1080del]	2, 2	p.[Pro193Ala]+[Lys359Argfs*14]
AGS430	Spanish	2A[a], M, F	−	c.[577C>G]+[2675G>A]	2, 9	p.[Pro193Ala]+[Arg892His]
AGS474	European-American	1A, M, F	−	c.3019G>A (het, *de novo*)	11	p.Gly1007Arg

A, affected individual; M, mother; F, father; het, heterozygous; hom, homozygous.

[a] Identical twins.